Evidence for General Nature of Pore Interconnectivity in 2-Dimensional Hexagonal Mesoporous Silicas Prepared Using Block Copolymer Templates

Sang Hoon Joo,[†] Ryong Ryoo,*[,†] Michal Kruk,[†,‡] and Mietek Jaroniec*[,‡]

National Creative Research Initiative Center for Functional Nanomaterials and Department of Chemistry, School of Molecular Science-BK21, Korea Advanced Institute of Science and Technology, Taejon 305-701, Korea, and Department of Chemistry, Kent State University, Kent, Ohio 44242

Received: September 20, 2001; In Final Form: February 13, 2002

Two-dimensional (2-D) ordered mesoporous silicas were synthesized following the literature synthesis procedures using two different silica sources (tetraethyl orthosilicate and sodium silicate) and poly(ethylene oxide)−poly(propylene oxide)−poly(ethylene oxide) triblock copolymer template under acidic and neutral synthesis conditions. The resultant SBA-15 and MSU−H silicas exhibited highly ordered mesoporous structures and pore sizes in the range from 7.5 to 10 nm. The silicas prepared under acidic conditions were clearly microporous, as seen from comparative analysis of adsorption data, whereas the comparative analysis did not indicate microporosity for the silica prepared under neutral conditions. The ordered mesoporous silicas were used as templates for the synthesis of carbon inverse replicas, and in all cases, the 2-D hexagonally ordered mesoporous carbons of CMK-3 type were obtained. This provided a strong evidence that the presence of connecting pores between uniform, ordered, mesoporous channels of 2-D hexagonally ordered silicas synthesized using polymer or oligomer templates with poly(ethylene oxide) blocks is a common feature of such materials and not merely an exceptional behavior restricted to certain SBA-15 silicas prepared under acidic conditions from TEOS.

1. Introduction

Oligomeric and block-copolymeric templates have recently become very popular in the synthesis of silicas with 2-dimensional (2-D) hexagonal structures.[1−14] Their application allowed one to extend the range of pore sizes and to improve hydrothermal stability[3] of previously reported 2-D hexagonally ordered mesoporous silicas, such as MCM-41,[15] FSM-16,[16] or SBA-3,[17] synthesized using alkylammonium surfactants as structure-directing agents. All these materials were thought to exhibit 2-D hexagonal arrays of approximately cylindrical nonintersecting pores, although minor differences in the structure of the pore walls were suggested to exist, mostly because of the different synthesis conditions and pathways employed. Nonetheless, the pores were widely believed to be disconnected for 2-D hexagonal silicas, as confirmed in the case of MCM-41 via imaging of platinum nanowires formed inside the pores,[18,19] or polymer,[20] platinum,[19] and carbon nanowires[21,22] isolated from the MCM-41 template. Recently, we have demonstrated that SBA-15 silica synthesized using poly(ethylene oxide)−poly(propylene oxide)−poly(ethylene oxide) (EO_nPO_m-EO_n) triblock copolymer exhibits a 2-D hexagonally ordered mesopore structure with interconnected pores.[23,24] This is clear from the fact that the synthesis of platinum and carbon in the SBA-15 structure readily results in the formation of 2-D hexagonally ordered platinum[24,25] and carbon[26,27] nanostructures that retain the 2-D hexagonal order upon the SBA-15 template removal. As already mentioned, the ordered nanostructures are not formed when MCM-41 template is used; separate nanowires or bundles of nanowires without retention of long-range 2-D hexagonal ordering are obtained.[25] We explained the formation of interconnected pore structure as a result of penetration of poly(ethylene oxide) blocks of the triblock copolymer in the siliceous pore walls of as-synthesized SBA-15.[23,24] We further suggested that other siliceous and perhaps even non-siliceous materials templated by polymers with EO_n blocks may exhibit connecting pores in the pore walls of the primary mesopores.[24] The presence of such pores would have a major impact on the application of 2-D hexagonally ordered polymer-templated silicas and other polymer-templated ordered mesoporous materials as lasing devices,[28] waveguides,[28] and templates for nanowire formation,[24−26,29−33] since the unidirectional nature of waveguiding could be compromised and the interconnectivity of nanowires could be developed in such 3-D connected porous systems.

The current study was intended to determine whether the 2-D hexagonally ordered pore system with connecting pores in pore walls is a feature specific to SBA-15 silica prepared under acidic conditions from tetraethyl orthosilicate (TEOS) or is a general feature of polymer-templated 2-D hexagonal mesoporous silicas. Therefore, 2-D hexagonally ordered silicas were synthesized from sodium silicate under acidic[7] and neutral[9] conditions. Inverse carbon replicas of the silicas were synthesized using the procedure originally proposed by Ryoo et al.[34] In all cases, the carbon inverse replication afforded 2-D hexagonal ordered carbons (CMK-3 type[26]), revealing the connectivity of ordered mesopores of the polymer-templated silicas. Because of the fact that carbon inverse replication[21,22,26,27,34−41] is a proven method for assessment of pore connectivity,[21,22,37,39,41] this result strongly suggests that 2-D hexagonally ordered silicas templated by polymers with EO_n blocks in general exhibit interconnected pores independently of conditions used for the synthesis and

* Profs. R. Ryoo and M. Jaroniec. E-mail: rryoo@mail.kaist.ac.kr and jaroniec@columbo.kent.edu. respectively.
[†] Korea Advanced Institute of Science and Technology.
[‡] Kent State University.

10.1021/jp013583n CCC: $22.00
Published on Web 04/05/2002

are thus conspicuously different from MCM-41 silicas with disconnected pores.

2. Materials and Methods

2.1. Materials. Three kinds of polymer-templated 2-D hexagonally ordered silicas were synthesized, following reported procedures[2,7,9] except for the modification of the starting composition and stirring mode. The first silica sample (designated as S1) was synthesized using TEOS (98% Acros) as a silica source under acidic condition[2] as follows: 4.0 g of Pluronic P123 was dissolved in 150 g of 1.6 M HCl solution. To this solution 8.50 g of TEOS was added, and the resulting mixture was stirred until TEOS was completely dissolved. The mixture was placed in an oven for 24 h at 308 K and then for 12 h more at 373 K under static condition. The second sample (S2) was synthesized using a sodium silicate solution (11.3% $Na_2Si_4O_9$ and 88.7% H_2O)[7] under acidic condition. Sodium silicate solution (27.6 g) was added to 126 g of 2.1 M hydrochloric acid containing 4 g of P123 at 308 K. The reactant mixing and subsequent thermal treatments were performed in the same manner as for S1. The synthesis of the third silica sample (S3) was carried out with the same sodium silicate solution but under neutral pH[9] as follows: 4.0 g of P123 was dissolved in 148 g of $1.4 \cdot 10^{-2}$ M HCl. Sodium silicate (27.6 g) was added to this solution, and the resulting mixture was stirred for 30 min at 308 K. The reaction mixture was kept at 308 K for 15 h without agitation and subsequently heated for 24 h at 373 K. All silica products were filtered, dried (without washing), and calcined at 823 K.

The carbon replication was performed with sucrose as described in detail elsewhere.[26] Briefly, the calcined silicas were infiltrated twice with sucrose solution containing sulfuric acid catalyst. The carbonization was carried out with heating to 1173 K under vacuum. The carbon−silica composites thus obtained are denoted SC*n* (with $n = 1-3$). The SC*n* samples were washed with hydrofluoric acid at room temperature, giving carbon samples denoted C*n*.

2.2. Measurements. X-ray diffraction (XRD) patterns were recorded on a Rigaku D/MAX-III instrument (operated at 3 kW) using Cu Kα radiation. Nitrogen adsorption measurements were performed at 77 K on a Micromeritics ASAP 2010 volumetric adsorption analyzer. Before the adsorption measurements, the samples were outgassed for 2 h at 473 K in the degas port of the adsorption analyzer. Weight change curves were recorded on a TA Instruments TGA 2950 high-resolution thermogravimeter under air atmosphere in the high-resolution mode with maximum heating rate of 20 K min^{-1}.

2.3. Calculations. The BET specific surface area[42] was calculated using adsorption data in the relative pressure range from 0.04 to 0.2. The total pore volume was determined from the amount adsorbed at a relative pressure of about 0.99. The external surface area and the pore volume were assessed using the α_s plot method[43] in the α_s range from 2 to 2.5 for silicas, and from 1.7 to 2.2 for carbons and carbon−silica composites (expect SC2, for which the range from 1.5 to 2.0 was used). The standard reduced adsorption for the reference adsorbent, α_s, is defined as an amount adsorbed at a given pressure divided by the amount adsorbed at a relative pressure of 0.4. The reference adsorption isotherm for silica[43] was used in the α_s plot analysis of the ordered mesoporous silicas, whereas the reference adsorption isotherm for carbon black[44] was used for ordered mesoporous carbons and carbon−silica composites. In the case of silicas, the pore volume that can be determined using the α_s plot method as described above is the sum of the volume of primary (ordered) mesopores and complementary micropores (and small mesopores). In the case of carbons, this pore volume is a sum of the volume of micropores and primary (ordered) mesopores, but may also contain a contribution from mesopores up to about 2−3 times as large as the primary mesopores. The latter pores are probably attributable to structural defects in ordered mesoporous carbon structure, as will be discussed later. In the case of carbon-silica composites, the pore volume is constituted by the micropore volume as well as the volume of ordered mesopores, if any, that have not been filled with carbon. It should be noted that the pores are classified herein as micropores (diameter below 2 nm), mesopores (diameter between 2 and 50 nm), and macropores (diameter above 50 nm).[42] The micropore volume for silicas was assessed using the α_s plot method in the α_s range from 0.9 to 1.2. The pore size distribution (PSD) was calculated using an algorithm based on the ideas of Barrett et al., but without the simplifying assumptions proposed by these authors.[45] The calculations were performed from adsorption branches of isotherms using the relations between the pore diameter and the capillary condensation pressure derived by Kruk et al. (KJS).[46] The statistical film thickness curve suitable for these calculations was reported elsewhere.[43] The KJS pore size is defined as a maximum of the KJS pore size distribution. In addition, the pore size, w_d, for ordered mesoporous silicas were evaluated using a geometrical equation proposed elsewhere for 2-D hexagonally ordered materials with honeycomb structure of uniform channel-like pores and with micropores in the pore walls:[47]

$$w_d = c d_{100} \left(\frac{V_p}{1/\rho + V_p + V_{mi}} \right)^{1/2} \quad (1)$$

where c is a constant characteristic of pore geometry and equal to 1.213 for cylindrical pores, d_{100} is the (100) interplanar spacing, ρ is the pore wall density (assumed to be equal to that for amorphous silica, that is 2.2 g cm^{-3}), V_{mi} is the volume of micropores in the pore walls, and V_p is the volume of primary (ordered) mesopores. V_{mi} was assessed from the α_s plot analysis, as described above, whereas V_p was assessed as a difference between the pore volume assessed from the α_s plot analysis (for α_s from 2.0 to 2.5) and the micropore volume. Due to a problem with an accurate measurements at very low angles on the diffractometer used, the angular position of the (100) peak was somewhat uncertain, and therefore, d_{100} was estimated from d_{200} interplanar spacing as follows: $d_{100} = 2d_{200}$.

3. Results and Discussion

3.1. Ordered Mesoporous Silicas. As can be seen is Figure 1, XRD patterns for calcined silicas are characteristic of 2-D hexagonal structures of high degree of ordering.[2,15−17] Similar XRD patterns have been reported for materials prepared under the synthesis conditions analogous to those employed herein.[2,7,9] The unit-cell parameters (evaluated from the (200) interplanar spacing: $a = 4 \cdot 3^{-1/2} d_{200}$) are listed in Table 1. Similar XRD patterns were recorded for as-synthesized materials, but the latter had the unit-cell parameter larger by 9%, 11%, and 4%, for samples S1, S2, and S3, respectively. This shows that the sample synthesized using sodium silicate under neutral conditions experienced the lowest degree of shrinkage upon calcination. This material also had the largest unit-cell size.

Nitrogen adsorption isotherms for the silicas are shown in Figure 2, and the pore structure parameters derived from adsorption data are listed in Table 1. Samples S1 and S2 exhibited adsorption isotherms similar to those reported previ-

TABLE 1: Structural Properties of Ordered Mesoporous Silica and Carbon Samples[a]

sample	a (nm)	S_{BET} (m^2 g^{-1})	V_t (cm^3 g^{-1})	S_{ex} (m^2 g^{-1})	$V_p + V_{mi}$ (cm^3 g^{-1})	w_{KJS} (nm)	w_d (nm)
S1	10.0	800	0.92	20	0.88	7.8	8.2
S2	10.0	580	0.76	50	0.67	7.9	7.9
S3	10.9	550	1.08	100	0.93	10.6	9.4
C1	9.4	1480	1.39	80	1.26[b]	4.6	c
C2	8.9	1200	1.07	50	0.96	4.5	c
C3	9.7	1060	0.91	40	0.84[b]	4.4	c

[a] Notation: a, unit-cell parameter determined from XRD (200) interplanar spacing; S_{BET}, BET specific surface area; V_t, total pore volume; S_{ex}, external surface area; $V_p + V_{mi}$, the sum of the primary mesopore volume and micropore volume; w_{KJS}, pore diameter evaluated using the KJS method; w_d, pore diameter evaluated from geometrical considerations (eq 1). [b] Includes the volume of pores that can be regarded as defects in ordered mesoporous structure. [c] See text for discussion.

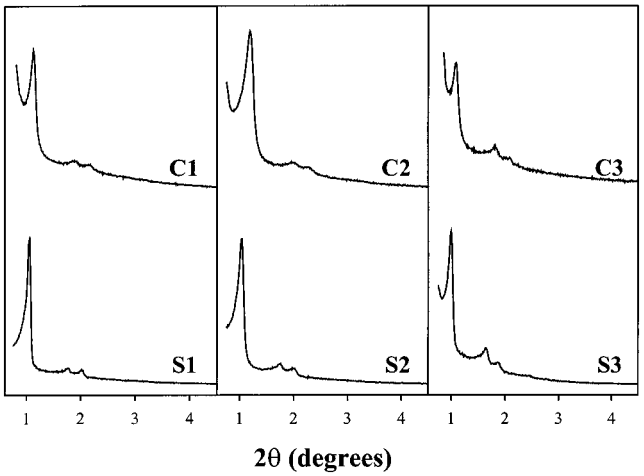

Figure 1. XRD patterns for the 2-D hexagonally ordered silica templates and their inverse carbon replicas.

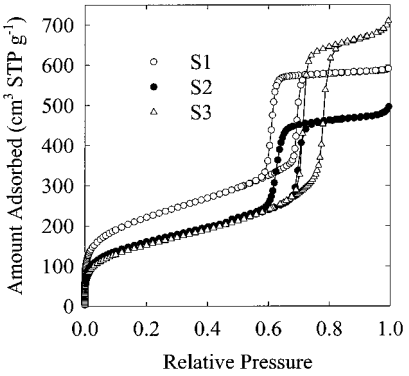

Figure 2. Nitrogen adsorption isotherms for the 2-D hexagonally ordered silicas.

ously for SBA-15 silicas synthesized from TEOS under acidic conditions,[2] and for MSU−H silicas synthesized from sodium silicate under neutral conditions in a one-step procedure.[14] In the case of these adsorption isotherms, more than half of the maximum adsorbed amount was attained before the onset of capillary condensation, the capillary condensation was sharp, and the isotherm leveled off at higher relative pressures. The silica prepared from sodium silicate (sample S2) exhibited the unit-cell size, which was somewhat smaller than that of the reported sample prepared under similar conditions,[7] but the BET specific surface areas of these two materials were highly similar. The silica prepared from sodium silicate under neutral conditions (sample S3) had the unit-cell size and total pore volume somewhat smaller than those for an MSU−H silica synthesized under similar conditions (that is, in a two-step procedure with initial synthesis temperature of 308 K),[14] but the specific surface areas of these two materials were similar. In fact, the adsorption isotherm for sample S3 is quite unusual for polymer-templated

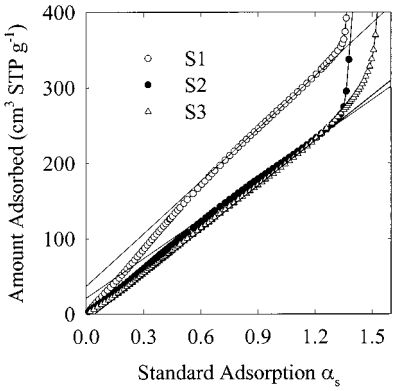

Figure 3. Initial parts of α_s plots for the 2-D hexagonally ordered silicas.

2-D hexagonally ordered silicas, because the increase in adsorption in the capillary condensation range is relatively large in comparison to the amount adsorbed before the onset of the capillary condensation step. This behavior is similar to that of some SBA-15 silicas calcined at high temperatures (1173 K or higher)[24,48] and indicative of low content of complementary micropores, or perhaps even their absence. This isotherm is different from that for other MSU−H silicas reported to date, which exhibited either isotherms similar to those for typical SBA-15[2] or isotherms with a considerable increase in adsorption after the completion of capillary condensation,[14] which is attributable to the existence of extensive interparticle (textural) porosity.

The comparative plot analysis indicated that samples S1 and S2 had appreciable amounts of micropores (0.06 and 0.03 cm^3 g^{-1}, respectively), whereas no indication of microporosity was found from the comparative plot analysis of sample S3, as its α_s plot was approximately linear for low α_s values (that is, for data corresponding to the low-pressure range) (see Figure 3). It should be noted that earlier studies[23,24,48] indicated that the comparative plot analysis is likely to underestimate the micropore volume for SBA-15 type materials. The pore size distributions calculated using the KJS method also indicated the presence of complementary micropores (and small mesopores) in the case of samples S1 and S2, and a lower content of complementary pores for sample S3 (see Figure 4). It is noted that the comparison of the KJS pore sizes[46] with those estimated using eq 1 indicated that the KJS pore sizes were quite accurate for samples S1 and S2, which had smaller pore sizes, whereas the KJS pore size of sample S3 with larger pores was overestimated by about 1 nm. A similar behavior was observed in a previous study.[14] Both of these results suggest that the extrapolation of the pore size−capillary condensation pressure relation proposed in the initial KJS work[46] for pores larger than 6.5 nm is good up to about 8−9 nm, and then becomes less accurate. Further studies are expected to allow for the improve-

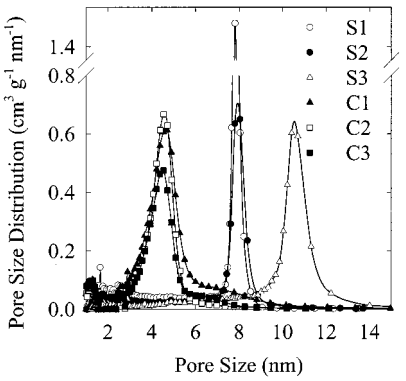

Figure 4. Pore size distributions for the 2-D hexagonally ordered silica and their carbon inverse replicas.

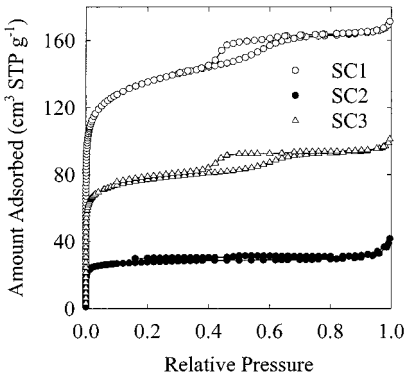

Figure 5. Nitrogen adsorption isotherms for the silica/carbon composites.

ment of the extrapolation used in the KJS procedure to extend its strict accuracy beyond pore sizes of 8−9 nm. It should be noted that the micropore volume used in calculations based on eq 1 is likely to be somewhat underestimated as mentioned above, and therefore the pore sizes calculated using eq 1 may be slightly overestimated.

It was suggested elsewhere[24,39] that the relationship between the size, surface area, and volume of primary pores can serve as a useful indication of the presence or absence of connecting pores in 2-D hexagonal structures. The estimate of the primary pore diameter (w) can be obtained using eq 1 (w_d) or the KJS method (w_{KJS}). The estimate of the primary pore surface area (S) can be obtained as a difference between the BET specific surface area (S_{BET}) and the external surface area (S_{ex}). The primary pore volume (V) (that is, the volume of primary mesopores and micropores, if any) can be assessed from the α_s plot method, as already described. When these methods are employed, wS/V assumes the value of about 4.5−5.0 for 2-D hexagonally ordered silicas without connecting pores (such as MCM-41 silica as well as SBA-15 silica subjected to calcination at temperatures above about 1173 K), whereas wS/V values above 5 are indicative of the presence of connecting pores.[39] These wS/V values deviate somewhat from the values of 4.0 and 4.2 expected for pores of cylindrical and hexagonal shapes, respectively.[24,48] This deviation is expected to be largely caused by the fact that the BET method employed for adsorption data in a typical relative pressure range (such as 0.04−0.2 used herein) under assumption of nitrogen molecule cross-sectional area of 0.162 nm^2 significantly overestimates the specific surface area for silicas (for discussion, see Kruk and Jaroniec[49]). In the case of the samples under current study, wS/V was 7.3, 6.2, and 4.6 for S1, S2, and S3 samples, respectively, when eq 1 was used to estimate the pore diameter (values of 6.9, 6.2, and 5.2 were obtained, respectively, when the KJS method was used). On the basis of these values, one can expect that samples S1 and S2 have 2-D hexagonal structure with 3-D pore connectivity, whereas S3 has a system of disconnected pore channels. In the latter case, it is expected that eq 1 provides a more reliable pore size assessment, and the wS/V value of 4.6 is more reliable than the value of 5.2 obtained using the pore size assessed using the KJS method. It should be noted that the latter value could serve as the basis of an expectation that there are some connecting pores present also in the S3 sample. Although this expectation will later be confirmed, it is not likely that the value of $wS/V = 5.2$ is more correct than 4.6. Instead, it will be suggested that the discrimination of the presence or absence of connecting pores based solely on wS/V ratio is too crude to be an unequivocal prediction tool.

3.2. Carbon/Silica Composites. SC1, -2, and -3 samples exhibited carbon/silica weight ratios of 0.50:1, 0.63:1, and 0.77:1, respectively, as inferred from TGA (it is assumed that the residue at 1273 K under air is the weight of silica, whereas the weight loss between 373 and 923 K corresponds to the weight of carbon). This provides the carbon weight/primary pore volume ratios of 0.57, 0.94, and 0.83 g of carbon per 1 cm^3 of the primary pore volume of the silica template. It should be noted that the template shrinks during carbonization required to obtain the silica/carbon composites, and therefore these loadings provide only a crude estimate of the exact carbon loadings per pore volume of the shrunken template, which are expected to be somewhat higher than those provided above. Nonetheless, the above loadings are likely to provide the means to compare the degree of carbon infiltration in these samples. This is clear from the fact that the adsorption capacity of the SC samples (see Figure 5 for nitrogen adsorption isotherms) is inversely proportional to this measure of the degree of infiltration, which is reasonable, since the more carbon fills the pores of the template, the less void space is accessible in these partially filled pores, and the smaller the adsorption capacity of the silica/carbon composite is. It is also interesting to note that the nitrogen adsorption isotherms for SC1 and SC3 samples exhibit residual amounts of accessible primary porosity, indicating that the infiltration with carbon is somewhat nonuniform in some pore parts.

3.3. Inverse Carbon Replicas. The inverse carbon replicas were stable under air atmosphere up to about 700 K, but they essentially completely burned out at higher temperatures (maximum rate of weight loss as the temperature increases was recorded at 763−776 K). The residue at 1273 K, which can be identified as the silica left after removal of the template, was equal to or below 3 wt %. As can be seen in Figure 1, all inverse carbon replicas exhibited 2-D hexagonal ordering, thus being ordered mesoporous carbons of CMK-3 type.[26] It should be noted that similar results for the inverse carbon replication of a sample synthesized from sodium silicate under nearly neutral conditions (that is, under conditions similar to those used for sample S3) have been reported[50] after submission of this work. The unit-cell sizes of the inverse replicas were 6%, 11%, and 11% smaller for C1, 2, and 3, respectively, than those of the silica templates used (see Table 1). Nitrogen adsorption isotherms of these carbons were similar to that originally reported for CMK-3 carbon,[26] featuring capillary condensation steps at relative pressures of about 0.45, which corresponds to the primary mesopore size of about 4.5 nm (see Figure 6 and Table 1).

It is interesting to note that because of the ordering of the CMK-3 structure, one can derive an equation that would allow

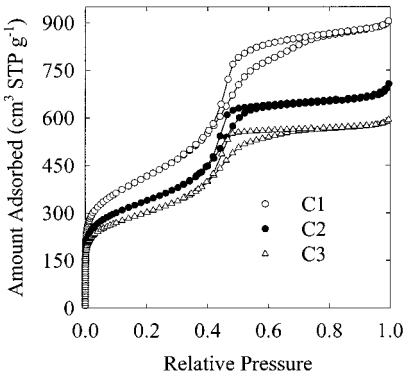

Figure 6. Nitrogen adsorption isotherms for the carbon inverse replicas of the 2-D hexagonally ordered silicas.

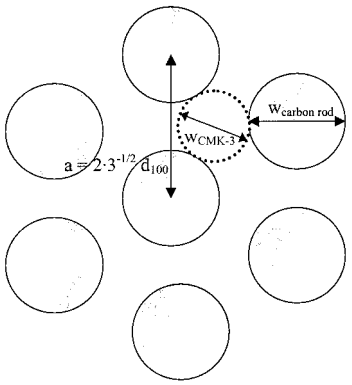

Figure 7. A schematic representation of a cross section through 2-D hexagonally ordered structure of CMK-3 carbon in the direction perpendicular to the axis of carbon rods. The existence of connectivity between the carbon rods was neglected.

one to estimate its primary mesopore size on the basis of selected structural parameters determinable from XRD and gas adsorption. CMK-3 carbon is an inverse replica of the SBA-15 structure, for which eq 1 is applicable. Therefore, the diameter of carbon rods can be estimated simply by making the following substitutions in eq 1. The primary pore volume in eq 1 should be replaced by the specific volume of carbon rods, the latter being equal to the sum of the specific volume of carbon framework ($1/\rho$, where ρ is the density of amorphous carbon) and the volume of micropores in the framework (V_{mi}). The volume of microporous pore walls ($1/\rho + V_{mi}$) in eq 1 should be substituted by the primary pore volume of CMK-3 (V_p). This leads to the following expression for the diameter of carbon rods in the CMK-3 structure:

$$w_{\text{carbon rod}} = cd_{100}\left(\frac{1/\rho + V_{mi}}{V_p + 1/\rho + V_{mi}}\right)^{1/2} \qquad (2)$$

where c is the same constant as that in eq 1, and d_{100} is (100) interplanar spacing in the CMK-3 structure. It is assumed that the carbon rods are circular, but the same expression is obtained if one assumes that the rods are hexagonal and their diameter is defined as the diameter of a circle of the same area as that of the cross section of the hexagonal rod. It should be noted that the presence of connections between the rods was neglected in this derivation, and consequently, it is not accounted for in the equation for the CMK-3 pore diameter (eq 3, see below) obtained from eq 2.

On the basis of the carbon rod diameter (eq 2) and the distance between the rods, one can calculate the size of primary mesopores of CMK-3. The primary pores of CMK-3 constitute a 3-D interconnected space between the 2-D hexagonally ordered carbon rods (see Figure 7). We can consider as a single pore the void confined between three adjacent rods that form a triangular arrangement, keeping in mind that such a single pore is connected to three adjacent pores of the same shape through the slits formed between two adjacent carbon rods. Let us define the size of such a single pore as a diameter of a cylinder inscribed between three adjacent carbon rods, as shown in Figure 7. It can be shown that in this case the CMK-3 pore diameter (defined as above and denoted w_{CMK-3}) is equal to $2 \cdot 3^{-1/2}a - w_{\text{carbon rod}}$, which can also be expressed as:

$$w_{CMK-3} = d_{100}\left[4/3 - c\left(\frac{1/\rho + V_{mi}}{V_p + 1/\rho + V_{mi}}\right)^{1/2}\right] \qquad (3)$$

In practice, an application of eq 3 is quite difficult because of the problems in determination of the micropore volume for ordered mesoporous carbons.[22] The presence of secondary pores of size close to the primary mesopore size may also cause problems in the determination of the primary mesopore volume for some of the CMK-3 samples (see below). Since C2 carbon is essentially free of these secondary pores, the use of eq 3 is demonstrated for this sample. It is assumed that the density of the carbon framework is equal to 2.05 g cm^{-3} (for justification, see Kruk et al.[22]) and the micropore volume is equal to 0.2 cm^3 g^{-1}. Under these assumptions, w_{CMK-3} is equal to 3.9 nm, which is quite close to the estimate from the KJS method (4.5 nm). Taking into account that the pores of CMK-3 carbon largely deviate from the cylindrical pore shape assumed in the KJS method, this agreement can be regarded as good and indicative of the applicability of eq 3 in pore size estimations of CMK-3 carbons. It should be noted that for the other two carbons considered, the use of eq 3 would require an additional assumption about the volume of primary mesopores, because this volume is difficult to separate from the volume of the aforementioned secondary pores. Therefore, the use of eq 3 was not attempted in this case.

For C1 and C3 carbons, the capillary condensation steps were followed by a region of less steep increase in the amount adsorbed before the adsorption isotherms finally leveled off at a relative pressure of about 0.75. This increase in the amount adsorbed corresponds to pores of size up to about 10 nm (see Figure 6), which can be speculated to be defects in the ordered structure of the material. Since CMK-3 type carbons are systems of interconnected, uniformly spaced rods, defects may have a form of (i) an indentation or hole in a carbon rod or (ii) a rod that is not connected (partially or fully) with the adjacent rods in a usual orderly way, but instead is inclined in the direction of some of the adjacent rods and perhaps has direct contact with the surface of these rods. These types of defects would create pores of size larger than those typical for the CMK-3 structure, which are interstices between ordered rods (see Figure 7). As noted above, C2 carbon is essentially free of these defects. The specific surface area and primary pore volume of the carbons under study are similar to those previously reported for CMK-3 type carbons.[26,39] The relatively large uptake of nitrogen at pressures preceding the capillary condensation suggests that these carbons exhibit micropores in the carbon framework, which is a well-known feature of ordered mesoporous carbons reported to date.[26,34]

The formation of ordered inverse carbon replicas of CMK-3 type for all of the silica templates used herein strongly suggests that the interconnectivity in the pore structure of 2-D hexagonal silicas templated by block copolymer surfactants exists independently of silica sources and synthesis conditions employed.

This result is not unexpected in the light of our earlier suggestion[23,24] that the interconnected porosity develops as a result of the penetration of EO_n blocks of the polymer template within the silica framework of as-synthesized polymer/silica composites. The tendency of EO_n blocks to this penetration is well documented in the literature.[51,52] The recent reports[53,54] of occurrence of microporosity in polymer-templated silicas with structures different from that of SBA-15 additionally confirm this interpretation. Therefore, one can expect that all or at least many of the polymeric-templated and probably also oligomeric-templated 2-D hexagonal silicas reported to date[1−14] exhibit interconnected pore systems of SBA-15 type. To this end, an evidence for the interconnected nature of 2-D hexagonal silicas synthesized using oligomeric templates has just been reported.[55] We have already discussed elsewhere that the comparative plot analysis is not capable of discriminating between materials with or without interconnecting pores,[48] which largely invalidates some earlier claims about the lack of connecting pores in SBA-15 silicas prepared under certain synthesis conditions.[56,57] Moreover, the current case of S3 sample that was expected to have essentially no connecting pores based on the wS/V ratio[24,39,48] shows the limitations of the analysis of the wS/V ratio, although the latter analysis can be a useful tool for a preliminary pore connectivity assessment.[39] It is recommended that conclusions about the pore connectivity in 2-D hexagonally ordered silicas should be made primarily on the basis of studies of carbon[34] or platinum[25] inverse replicas of these silicas. Gas adsorption data can certainly serve as a useful tool for crude prediction of the possibility of existence of pore connectivity, but conclusions derived from them cannot be treated as definite and final.

4. Conclusions

As revealed by the inverse carbon replication, the triblock-copolymer-templated 2-D hexagonally ordered silicas prepared from two different silica sources (TEOS and sodium silicate) under both acidic and neutral conditions all exhibit interconnected porous systems (we propose to generally refer to this structure type as SBA-15 type). This result strongly suggests that 2-D hexagonally ordered silicas templated by polymers (and most likely also by oligomers) with poly(ethylene oxide) blocks tend to be of SBA-15 type and thus should not be claimed to have disconnected pore systems or to be MCM-41 analogues, unless firm evidence, preferably from carbon or platinum replication, is produced. This tendency to form connecting pores in the walls of ordered primary pores of silicas templated by polymeric templates appears to related to the propensity of poly(ethylene oxide) blocks to interact with silicate walls and interpenetrate them. This tendency may also extend upon non-siliceous ordered porous materials templated by polymers and oligomers.[58] It is certainly worthwhile to investigate the pore connectivity in other oligomer- and polymer-templated 2-D hexagonal silicas reported to date to determine whether there are exceptions from the SBA-15 type behavior or this behavior is universal for such silicas. It is already known that SBA-15 silicas can potentially be transformed into MCM-41 analogues via high-temperature calcination at temperatures above about 1173 K,[39] but the assessment of the success of such a transformation is expected to be very difficult without resorting to replication procedures. It is important to identify or develop other ways in which MCM-41 analogues can be synthesized using polymeric or oligomeric templates.

The current study demonstrated that CMK-3 carbons can be synthesized using silica templates produced from cost-effective reagents, including sodium silicate (instead of an expensive TEOS), confirming and extending the results of another recent study.[50] This largely facilitates a prospective large-scale production of ordered mesoporous carbons, because both silica templates and carbon frameworks can now be synthesized using cheap reagents.

Acknowledgment. This work was supported in part by the Ministry of Science and Technology through Creative Research Initiative Program (R.R.), by School of Molecular Science through Brain Korea 21Project (R.R.), and by the donors of the Petroleum Research Fund administered by the American Chemical Society (M.J.).

References and Notes

(1) Attard, G. S.; Glyde, J. C.; Goltner, C. G. *Nature* **1995**, *378*, 366.
(2) Zhao, D.; Feng, J.; Huo, Q.; Melosh, N.; Fredrickson, G. H.; Chmelka, B. F.; Stucky, G. D. *Science* **1998**, *279*, 548.
(3) Zhao, D.; Huo, Q.; Feng, J.; Chmelka, B. F.; Stucky, G. D. *J. Am. Chem. Soc.* **1998**, *120*, 6024.
(4) Zhang, W.; Glomski, B.; Pauly, T. R.; Pinnavaia, T. J. *Chem. Commun.* **1999**, 1803.
(5) Bagshaw, S. A. *Chem. Commun.* **1999**, 271.
(6) Boissiere, C.; Larbot, A.; van der Lee, A.; Kooyman, P. J.; Prouzet, E. *Chem. Mater.* **2000**, *12*, 2902.
(7) Kim, J. M.; Stucky, G. D. *Chem. Commun.* **2000**, 1159.
(8) Kim, J. M.; Han, Y.-J.; Chmelka, B. F.; Stucky, G. D. *Chem. Commun.* **2000**, 2437.
(9) Kim, S.-S.; Pauly, T. R.; Pinnavaia, T. J. *Chem. Commun.* **2000**, 1661.
(10) Bagshaw, S. A. *J. Mater. Chem.* **2001**, *11*, 831.
(11) Coleman, N. R. B.; Attard, G. S. *Microporous Mesoporous Mater.* **2001**, *44*−*45*, 73.
(12) Sun, J.-H.; Moulijn, J. A.; Jansen, J. C.; Maschmeyer, T.; Coppens, M.-O. *Adv. Mater.* **2001**, *13*, 327.
(13) Blin, J. L.; Leonard, A.; Su, B. L. *Chem. Mater.* **2001**, *13*, 3542.
(14) Kim, S. S.; Karkamkar, A.; Pinnavaia, T. J.; Kruk, M.; Jaroniec, M. *J. Phys. Chem. B* **2001**, *105*, 7663.
(15) Beck, J. S.; Vartuli, J. C.; Roth, W. J.; Leonowicz, M. E.; Kresge, C. T.; Schmitt, K. D.; Chu, C. T−W.; Olson, D. H.; Sheppard, E. W.; McCullen, S. B.; Higgins, J. B.; Schlenker, J. L. *J. Am. Chem. Soc.* **1992**, *114*, 10834.
(16) Inagaki, S.; Fukushima, Y.; Kuroda, K. *J. Chem. Soc., Chem. Commun.* **1993**, 680.
(17) Huo, Q.; Margolese, D. I.; Ciesla, U.; Feng, P.; Gier, T. E.; Sieger, P.; Leon, R.; Petroff, P. M.; Schuth, F.; Stucky, G. D. *Nature* **1994**, *368*, 317.
(18) Ko, C. H.; Ryoo, R. *Chem. Commun.* **1996**, 2467.
(19) Liu, Z.; Sakamoto, Y.; Ohsuna, T.; Hiraga, K.; Terasaki, O.; Ko, C. H.; Shin, H. J.; Ryoo, R. *Angew. Chem., Int. Ed.* **2000**, *39*, 3107.
(20) Johnson, S. A.; Khushalani, D.; Coombs, N.; Mallouk, T. E.; Ozin, G. A. *J. Mater. Chem.* **1998**, *8*, 13.
(21) Lee, J.; Yoon, S.; Oh, S. M.; Shin, C.-H.; Hyeon, T. *Adv. Mater.* **2000**, *12*, 359.
(22) Kruk, M.; Jaroniec, M.; Ryoo, R.; Joo, S. H. *J. Phys. Chem. B* **2000**, *104*, 7960.
(23) Kruk, M.; Jaroniec, M.; Ko, C. H.; Ryoo, R. *Chem. Mater.* **2000**, *12*, 1961.
(24) Ryoo, R.; Ko, C. H.; Kruk, M.; Antochshuk, V.; Jaroniec, M. *J. Phys. Chem. B* **2000**, *104*, 11465.
(25) Shin, H. J.; Ko, C. H.; Ryoo, R. *J. Mater. Chem.* **2001**, *11*, 260.
(26) Jun, S.; Joo, S. H.; Ryoo, R.; Kruk, M.; Jaroniec, M.; Liu, Z.; Ohsuna, T.; Terasaki, O. *J. Am. Chem. Soc.* **2000**, *122*, 10712.
(27) Joo, S. H.; Choi, S. J.; Oh, I.; Kwak, J.; Liu, Z.; Terasaki, O.; Ryoo, R. *Nature* **2001**, *412*, 169.
(28) Yang, P.; Wirnsberger, G.; Huang, H. C.; Cordero, S. R.; McGehee, M. D.; Scott, B.; Deng, T.; Whitesides, G. M.; Chmelka, B. F.; Buratto, S. K.; Stucky, G. D. *Science* **2000**, *287*, 465.
(29) Huang, M. H.; Choudrey, A.; Yang, P. *Chem. Commun.* **2000**, 1063.
(30) Han, Y.-J.; Kim, J. M.; Stucky, G. D. *Chem. Mater.* **2000**, *12*, 2068.
(31) Kang, H.; Jun, Y.-w.; Park, J.-I.; Lee, K.-B.; Cheon, J. *Chem. Mater.* **2000**, *12*, 3530.
(32) Coleman, N. R. B.; Morris, M. A.; Spaldong, T. R.; Holmes, J. D. *J. Am. Chem. Soc.* **2001**, *123*, 187.
(33) Jang, J.; Lim, B.; Lee, J.; Hyeon, T. *Chem. Commun.* **2001**, 83.
(34) Ryoo, R.; Joo, S. H.; Jun, S. *J. Phys. Chem. B* **1999**, *103*, 7743.
(35) Lee, J.; Yoon, S.; Hyeon, T.; Oh, S. M.; Kim, K. B. *Chem. Commun.* **1999**, 2177.
(36) Yoon, S. B.; Kim, J. Y.; Yu, J.-S. *Chem. Commun.* **2001**, 559.

(37) Ryoo, R.; Joo, S. H.; Kruk, M.; Jaroniec, M. *Adv. Mater.* **2001**, *13*, 677.
(38) Joo, S. H.; Jun, S.; Ryoo, R. *Microporous Mesoporous Mater.* **2001**, *44*−*45*, 153.
(39) Shin, H. J.; Ryoo, R.; Kruk, M.; Jaroniec, M., *Chem. Commun.* **2001**, 349.
(40) Lee, J.; Sohn, K.; Hyeon, T. *J. Am. Chem. Soc.* **2001**, *123*, 5146.
(41) Jansen, J. C.; Shan, Z.; Marchese, L.; Zhou, W.; Puil, N. v. d.; Maschmeyer, T. *Chem. Commun.* **2001**, 713.
(42) Rouquerol, J.; Avnir, D.; Fairbridge, C. W.; Everett, D. H.; Haynes, J. H.; Pernicone, N.; Ramsay, J. D. F.; Sing, K. S. W.; Unger, K. K. *Pure Appl. Chem.* **1994**, *66*, 1739.
(43) Jaroniec, M.; Kruk, M.; Olivier, J. P. *Langmuir* **1999**, *15*, 5410.
(44) Kruk, M.; Jaroniec, M.; Gadkaree, K. P. *J. Colloid Interface Sci.* **1997**, *192*, 250.
(45) Barrett, E. P.; Joyner, L. G.; Halenda, P. P. *J. Am. Chem. Soc.* **1951**, *73*, 373.
(46) Kruk, M.; Jaroniec, M.; Sayari, A. *Langmuir* **1997**, *13*, 6267.
(47) Kruk, M.; Jaroniec, M.; Sayari, A. *Chem. Mater.* **1999**, *11*, 492.
(48) Matos, J. R.; Mercuri, L. P.; Kruk, M.; Jaroniec, M. *Chem. Mater.* **2001**, *13*, 1726.
(49) Kruk, M.; Jaroniec, M. *Chem. Mater.* **2001**, *13*, 3169.
(50) Kim, S.-S.; Pinnavaia, T. J. *Chem. Commun.* **2001**, 2418.
(51) De Paul, S. M.; Zwanziger, J. W.; Ulrich, R.; Wiesner, U.; Spiess, H. W. *J. Am. Chem. Soc.* **1999**, *121*, 5727.
(52) Melosh, N. A.; Lipic, P.; Bates, F. S.; Wudl, F.; Stucky, G. D.; Fredrickson, G. H.; Chmelka, B. F. *Macromolecules* **1999**, *32*, 4332.
(53) Smarsly, B.; Goltner, C.; Antonietti, M.; Ruland, W.; Hoinkis, E. *J. Phys. Chem. B* **2001**, *105*, 831.
(54) Goltner, C. G.; Smarsly, B.; Berton, B.; Antonietti, M. *Chem. Mater.* **2001**, *13*, 1617.
(55) Lee, J.-S.; Joo, S. H.; Ryoo, R. *J. Am. Chem. Soc.* **2002**, *124*, 1156.
(56) Imperor-Clerc, M.; Davidson, P.; Davidson, A. *J. Am. Chem. Soc.* **2000**, *122*, 11925.
(57) Miyazawa, K.; Inagaki, S. *Chem. Commun.* **2000**, 2121.
(58) Yang, P.; Zhao, D.; Margolese, D. I.; Chmelka, B. F.; Stucky, G. D. *Nature* **1998**, *396*, 152.